

This is an Open Access document downloaded from ORCA, Cardiff University's institutional repository: <https://orca.cardiff.ac.uk/id/eprint/121054/>

This is the author's version of a work that was submitted to / accepted for publication.

Citation for final published version:

Lissenberg, C. Johan , MacLeod, Christopher J. and Bennett, Emma N. 2019. Consequences of a crystal mush-dominated magma plumbing system: a mid-ocean ridge perspective. *Philosophical Transactions A: Mathematical, Physical and Engineering Sciences* 377 (2139) 10.1098/rsta.2018.0014

Publishers page: <http://dx.doi.org/10.1098/rsta.2018.0014>

Please note:

Changes made as a result of publishing processes such as copy-editing, formatting and page numbers may not be reflected in this version. For the definitive version of this publication, please refer to the published source. You are advised to consult the publisher's version if you wish to cite this paper.

This version is being made available in accordance with publisher policies. See <http://orca.cf.ac.uk/policies.html> for usage policies. Copyright and moral rights for publications made available in ORCA are retained by the copyright holders.



Consequences of a crystal mush-dominated magma plumbing system: a mid-ocean ridge perspective

C. Johan Lissenberg^{*}, Christopher J. MacLeod and Emma N. Bennett

*School of Earth and Ocean Sciences, Cardiff University
Park Place, Cardiff CF10 3AT, United Kingdom
ORCID ID: 0000-0001-7774-2297*

Keywords: crystal mush, mid-ocean ridge, magma chamber, mid-ocean ridge basalt

Summary

Crystal mush is rapidly emerging as a new paradigm for the evolution of igneous systems. Mid-ocean ridges provide a unique opportunity to study mush processes: geophysical data indicate that, even at the most magmatically robust fast-spreading ridges, the magma plumbing system is typically comprised of crystal mush. In this paper, we describe some of the consequences of crystal mush for the evolution of the mid-ocean ridge magmatic system. One of these is that melt migration by porous flow plays an important role, in addition to rapid, channelised flow. Facilitated by both buoyancy and (deformation-enhanced) compaction, porous flow leads to reactions between the mush and migrating melts. Reactions between melt and the surrounding crystal framework are also likely to occur upon emplacement of primitive melts into the mush. Furthermore, replenishment facilitates mixing between the replenishing melt and interstitial melts of the mush. Hence, crystal mushes facilitate reaction and mixing, which leads to significant homogenisation, and which may account for the geochemical systematics of mid-ocean ridge basalt. A second consequence is cryptic fractionation. At mid-ocean ridges, a plagioclase framework may already have formed when clinopyroxene saturates. As a result, clinopyroxene phenocrysts are rare, despite the fact that the vast majority of MORB records clinopyroxene fractionation. Hence, melts extracted from crystal mush may show a cryptic fractionation signature. Another consequence of a mush-dominated plumbing system is that channelised flow of melts through the crystal mush leads to the occurrence of vertical magmatic fabrics in oceanic gabbros, as well as the entrainment of diverse populations of phenocrysts. Overall, we conclude that the occurrence of crystal mush has a number of fundamental implications for the behaviour and evolution of magmatic systems, and that mid-ocean ridges can serve as a useful template for trans-crustal mush columns elsewhere.

*Author for correspondence

(lissenbergcj@cardiff.ac.uk).

1. Introduction

Magma chambers have traditionally been considered to be magma filled reservoirs, where melt evolution is controlled by the removal of crystals through crystal settling and/or crystallisation along the walls of the chamber. However, this view is now being challenged, and a new paradigm is emerging where magma reservoirs are considered to be filled predominantly by crystal mush (1-3). This paradigm shift was predominantly initiated by the realisation that melt-filled chambers are difficult to maintain over geologically significant periods of time, particularly in the upper continental crust, and by petrological observations (see (2) for a review). At mid-ocean ridges, the realisation that the plumbing system is dominated by crystal mush came relatively early, and was driven primarily by geophysical observations: the large melt-filled chambers once considered to underlay the ridge axis (4, 5) were not found by geophysical surveys in the 1980's (see (6) for a review). Instead, the data indicated the presence of crystal mush.

As discussed by (2), the emerging mush paradigm requires a reassessment of the processes controlling plutonic and volcanic evolution. The mid-ocean ridge magmatic system provides an ideal opportunity to do so. This is because it features a combination of observables that is difficult to find in other geodynamic settings: it is an active system, which enables geophysical data to constrain the nature of the magma plumbing system (e.g., (6)), yet both plutonic and volcanic sections are available for sampling. Hence, the plutonic-volcanic connection can be assessed directly, and the significance of petrological and geochemical observables can be placed within the framework of known magma chamber architecture. Furthermore, mid-ocean ridges do not suffer from complications introduced by the interaction of the magmatic system with older and compositionally different country rocks: all observables relate directly to the magmatic system itself.

In this paper, we use petrological observations on the mid-ocean ridge system to reflect on some of the consequences of a magma plumbing system dominated by crystal mush. We first cover the geophysical constraints on the nature of mid-ocean ridge magma chambers, and then discuss the role the crystal mush plays in melt transport, the compositional evolution of melts, and the generation of cryptic fractionation. We conclude that mush processes exert a fundamental control on the physical and chemical evolution of the mid-ocean ridge magmatic system.

2. The geophysical framework: a mush-dominated magma plumbing system

The nature of the mid-ocean ridge magma plumbing system is best constrained at the fast-spreading East Pacific Rise, where a wealth of seismic data has been obtained over the last three decades. Seismic reflection data have established that the top of the magmatic system is formed by a melt-bearing body 1-2 km below the seafloor, situated at the transition from the sheeted dykes to lower crustal gabbros (7-10). This so-called axial melt lens is hundreds of meters to a few kilometres wide, and tens of meters thick (9). It is present along a large proportion of the ridge axis (~85% at 9-10°N on the East Pacific Rise), but is not continuous, with numerous disruptions present, commonly associated with ridge axial discontinuities (11). Although the axial melt lens contains enough melt to possess a negative seismic velocity anomaly relative to the overlying sheeted dykes, more recent work has shown that the axial melt lens is not uniformly melt rich (12): it is segmented on a both a kilometre and hundreds of meters scale into crystal-rich and crystal-poor portions (13, 14). Furthermore, melt lens depth varies over short spatial scales (11, 15). Hence, the axial melt lens is a dynamic horizon, with changes in depth, melt and crystal proportions in both space and time.

The axial melt lens overlies a large region with attenuated seismic velocities. Seismic tomography and seafloor compliance data indicate that this region, referred to as the low-velocity zone, is typically ~7 km wide, and extends to the base of the crust at ~6 km depth (16-18). It is interpreted to be a crystal mush. Proportions of melt are difficult to determine and model-dependent, but estimates range from a few to potentially a few tens of percent (16, 17). Within the low-velocity zone, a number of melt lenses have been found in recent years (19). These occur both on axis and up to 8 km off-axis (20). Furthermore, a number of sills have been detected at the Moho (21). Overall, the seismic character of the East Pacific Rise changes little along the ridge axis, indicating that it approximates steady state over geological time.

Intermediate-spreading ridges, such as the Juan de Fuca Ridge, appear to have a similar seismic structure to fast-spreading ridges: they, too, feature a segmented axial melt lens with a variable crystal content (22, 23). However, the axial melt lens here is deeper than at the East Pacific Rise, indicating an overall cooler thermal structure. At slow-spreading ridges, mantle upwelling is sufficiently slow and cooling sufficiently efficient that a steady-state melt lens cannot be maintained, and a regular Pacific-type, 6 km thick layer-cake igneous crust may not form. Some segments (e.g., Vema) expose crust that appears to conform to the classic Penrose stratigraphy of gabbros-sheeted dykes-lavas, but the seismically-defined crustal thickness is variable along axis, and anomalously thin at the ends of ridge segments (24): such along-axis variation appears to be the norm at slow spreading rates (25). Other, less magmatically robust segments locally expose mantle peridotite, with

or without gabbroic intrusions, indicating that slow-spreading lithosphere along such segments may be composed of lithospheric mantle intruded by gabbroic plutons, such that a pure igneous crust does not form (26). Consistent with these observations, axial melt lenses are not normally present at slow-spreading ridges: so far they have only been detected at two locations on the Mid-Atlantic Ridge: at 57°N on the Reykjanes Ridge (27), and Lucky Strike (37°N), which is near the magmatically robust Azores platform (28). As at fast-spreading systems, the melt lens at Lucky Strike overlies a region of crystal mush. At other slow-spreading segments for which seismic data are available, only crystal mush has been detected (29, 30). Overall, these observations imply that the generally lower amount of melt supply and the cooler thermal structure at slow spreading rates lead to significant variations in the nature of the plumbing system: in contrast to fast-spreading ridges, the system is not in steady state. Instead, because of the generally cooler thermal structure, emplaced melts quickly turn to the observed mush bodies, and they cannot sustain an axial melt lens.

Overall, the seismic data of mid-ocean ridges indicate that the magma plumbing system is dominated by crystal mush (6).

3. Consequences of a mush-dominated magma plumbing system

The prominence of crystal mush in the plumbing system of mid-ocean ridges has a number of consequences for the magmatic processes occurring in the system, for which we may look for evidence in the rock record. In the sections below, we discuss a three of these: modes of melt transport, buffering of melt compositions and cryptic fractionation.

3.1. Melt transport

Melt transport mechanisms in crystal mush are predicted to differ from those in melt-filled magma chambers surrounded by solid wall rock. In the latter situation, melt transport can readily occur by dyking, particularly in a mid-ocean ridge setting, where extension creates optimum condition for dyke formation to occur. In contrast, in a crystal mush melts are predicted to migrate by porous flow (31), provided that the interstitial melt is positively buoyant with respect to the surrounding crystal framework. To determine whether melts are buoyant in a mid-ocean ridge crystal mush, we modelled the differentiation of a primitive MORB using MELTS v. 1.2 (32). We chose the proposed Indian Ocean primary melt of (33) (also modelled in (34); composition listed in Table S1),

assuming 0.15% H₂O, and simulated fractional crystallisation at 2 kbar. Although the exact crystallisation sequence will depend on the assumed melt composition, water content and pressure, most MORB will follow a similar crystallisation path, and we assume that the results in terms of density evolution are generally applicable. The results are shown in figure 1, which plots the density of the melt and the density of the bulk cumulate assemblage crystallised at each step as a function of temperature. As can be seen, the density of the melt at its liquidus is 2.68 g/cm³; in the temperature interval 1270°C-1120°C, where the majority of crystallisation occurs, melt density changes very little. Although the density of the fractionated crystals changes significantly as a function of the saturation temperatures of the different phases, the density of the melt is always below that of the crystals. Hence, melts in a mid-ocean ridge crystal mush are predicted to be positively buoyant throughout their crystallisation histories.

The upward migration of buoyant interstitial melts may be further aided by compaction. Although it has been suggested that compaction may not play as significant a role in generating cumulate rocks as once thought in all plutonic systems (35), we posit that, compared to continental-hosted intrusions, the lower oceanic crust provides an environment where compaction is most likely to occur. This is because: (i) the mush cools slowly, so that there is sufficient time for compaction to occur; (ii) interconnected mush thickness is as much as 4-5 km at fast-spreading ridges, providing a significant gravitational driving force; and (iii) the regime of continual intrusion coupled with wholesale bulk deformation of the system will all act to enhance the efficiency of melt expulsion. Evidence that compaction may indeed play a role in mid-ocean ridge mush systems is provided by three observations. The first is that minor deformation twins in plagioclase and kink bands in olivine are very common: an example is shown in figure 2. These structures are present even if they are not associated with any solid-state deformation, such as the fast-spreading East Pacific Rise, where solid-state deformation appears to be completely absent (36, 37) Hence, we argue that these textures result from the compaction of the crystal mush: compaction will lead to the mechanical interaction between different mineral grains as melt is expelled and the modal proportion of crystals increases (38, 39), leading to minor deformation of the crystal lattice through dislocation creep. Considering that the melt proportion in most of the mid-ocean ridge crystal mush is considered to be <20% (see section 2), such particle interaction appears inevitable. Particle interaction is also responsible for the second line of evidence for compaction: the occurrence of pressure solution driven by impingement of different grains (40). A final consideration is magmatic flow, which is expected to be common at mid-ocean ridges because of the continuous extension of the crust, and, at fast-spreading ridges,

because the lower crust is mechanically coupled to the flow of the underlying mantle as it rolls over beneath the ridge axis (41). Magmatic flow results in simple shear-dominated deformation of the crystal mush. As a result, it is common for oceanic plutonic rocks to be foliated and/or lineated (figure 2), and the same is true for plutonic rocks from the Oman ophiolite (36, 41-44). The fabrics in these rocks are defined by aligned crystals that contain no features characteristic of solid-state deformation, such as dislocation structures and subgrains (36). This indicates that the deformation occurred in the presence of melt (45, 46): i.e., deformation operated when the system was a crystal mush. If deformation occurs in a crystal mush, this will lead to expulsion and focusing of interstitial melts into melt-rich zones, thus facilitating melt segregation from the compacting crystal framework (47-49). Hence, although the degree to which compaction occurs in relatively small continental magma chambers remains an open question (35), the observations of the mid-ocean ridge crystal mush suggest that compaction is an important process in this setting.

Combined, the buoyancy forces and (deformation-assisted) compaction will lead to the upward migration of the interstitial melts by porous flow. The crystal framework through which the melts flow is highly variable in composition: although it will be dominated by a fairly simple mineral assemblage of olivine, plagioclase and clinopyroxene, observations from lower crustal sections across the spreading rate spectrum indicate that modal proportions and mineral compositions vary on a centimetre to metre scale (e.g., (33, 37, 50)). As a result, it is highly unlikely that percolating melts retain equilibrium with the mush framework during their ascent. This will lead to reactions between the melts and framework: hence, porous flow is expected to be reactive. A significant number of observations in the last decade have firmly established the footprint of this process in the mid-ocean ridge rock record (51-57). These have recently been covered in depth in (34), and we only recap the main findings here. The first is that evidence for reactions between crystal and migrating melt are nearly ubiquitously preserved in oceanic plutonic rocks (34) as well as lower crustal xenoliths in MORB (56, 57), and are manifest on a grain scale by both reaction textures (e.g., dissolution fronts, symplectites) and mineral compositions. From a compositional viewpoint, zoning in major elements of cumulus (i.e., former framework) crystals towards domains of melt flow is associated with unusual enrichment and fractionation of trace elements (54). The second main finding is that the same trace element enrichment and fractionation that is found on a grain scale also occurs on the scale of the entire lower crust (54). This suggests that the lower crustal crystal mush acts as one system, and that it is permeable throughout. This is consistent with the fact that the lower crust, at least at Hess Deep

in the Pacific, forms an overall upward differentiation sequence. Hence, the lower crustal crystal mush is an interconnected system, evolving upwards, with a significant role for reactive porous flow.

The consequences of reactive porous flow are profound: melt evolution no longer obeys the laws of fractional crystallisation. From a major element perspective, reactions may change the MgO-FeO-CaO-Al₂O₃ relationships, as these are the dominant elements in the main phases involved (53). MgO, in particular, is sensitive to reactive flow, as Fe-Mg exchange between migrating melts and crystals is rapid. In the case where evolved melts interact with a primitive matrix, this can lead to unusual mineral and melt compositions, with equilibration with the matrix leading to Mg# typical of a primitive melt composition, but enriched incompatible elements (e.g., Ti) (53). From a trace element perspective, it is striking that the reactive geochemical signature of trace element enrichment and fractionation that is present in the lower crust is very similar to the trace element distributions in MORB (54). This led (34) to argue that MORB trace element bear an imprint of reactive porous flow in the lower oceanic crust.

However, porous flow is unlikely to be the only melt transport mechanism operating in the lower oceanic crust. Observations in the Oman ophiolite, an analogue for fast-spreading oceanic crust, indicate that the sheeted dykes and lavas are in Fe-Mg equilibrium with cumulates from the deeper part of the lower crust, but not with those from the upper part of the lower crust (58). Similarly, the upper gabbros in Hess Deep are not in equilibrium with the overlying sheeted dykes and lavas (59). These data require that melts were extracted from the deeper parts of the lower crustal crystal mush without only limited interaction with the overlying, more evolved parts of the mush, and that extraction was rapid and efficient enough to transport melts upwards by several kilometres to erupt. Melt transport by porous flow would not satisfy either of these criteria.

Such rapid, channelised melt flow requires that melts can be efficiently extracted from the mush. One mechanism for this to occur is by concentrating (interstitial) melts into melt-rich zones. Such self-organisation may occur as a result of crystal setting and compaction, aided by deformation, as discussed above. This is consistent with numerical models of crystal mushes, which indicate that compaction of an internally homogeneous mush will lead to melt segregation and concentration (e.g., (60)). Once melts have segregated into a sufficiently large melt body, they may travel upwards through the mush as porosity waves (61, 62). Alternatively, their buoyancy may destabilise the overlying crystal mush, and melt rapidly travels to the top of the system (63). In addition to melt segregation, replenishment of the mush is likely to play a significant role in the occurrence of channelised melt transport. It is a very effective means of unlocking, or fluidizing, the mush, leading

to rapid upward transport of melts in crystal-poor ‘chimneys’ (64-66). Hence, processes that are inherent to replenished crystal mushes such as those of the lower oceanic crust may facilitate melts to be extracted and erupted.

From a mid-ocean ridge perspective, these dynamic processes operating in the crystal mush not only explain the occurrence of both porous and focused melt transport, but they may also facilitate magma mixing, provide an explanation for the presence of diverse populations of phenocrysts/antecrysts in MORB, and can account for observed magmatic fabrics. The role of replenishment and magma mixing in MORB is well documented (67-72), and is usually assumed to occur in melt-rich reservoirs. Within a crystal mush, mixing may occur between the replenishing melt and the interstitial melt present in the mush. In effect, this would produce effects akin to in-situ fractionation, where interstitial melts are returned to a melt reservoir in a static magma chamber crystallising inwards from its walls (73). In the mush variant discussed here, interstitial melt is mobilised from a crystal mush by the destabilising effect of replenishment (64, 66, 74-76). Either way, interstitial melts are mixed with a larger body of melt, so the geochemical affects are likely to be similar. It has been noted that the incompatible trace element distributions of MORB, which are over-enriched relative to fractional crystallisation predictions (54, 67) can be explained by in-situ fractionation (77), or, alternatively, by a contribution of trace element enriched interstitial melts to MORB (34, 54). Mush destabilisation by replenishment can account for either of these. It can also account for the observation that MORB commonly contains diverse populations of phenocrysts and antecrysts, each recording a different petrogenetic history (74-76, 78-80), as well as xenoliths of crystal mush (56, 57): when mush destabilises and melts are transported upwards through it, they may pick up crystals and crystal clots from different parts of the system. Furthermore, even when crystals originate from a single location, the dynamics of mixing of melt and mush can be such that each crystal may take a different composition-time path, leading to the generation of multiple populations (64). Finally, focused melt transport through a crystal mush may explain the occurrence of vertical magmatic fabrics in gabbros from the top third of fast-spreading lower oceanic crust. Such fabrics have been documented in both Pacific lower crust (36, 44) and in the Oman ophiolite (42, 81, 82), and are defined predominantly by aligned plagioclase defining both a sheeted dyke-parallel foliation and approximately vertical lineation. Although some workers argue that the fabrics record downward flow of cumulates produced in the overlying axial melt lens (e.g., (83-86)), the fact that the deeper, layered gabbros are more primitive than the foliated gabbros, and that, in contrast to the layered gabbros below, the foliated gabbros are not layered, makes this scenario unlikely. Instead, we

argue that the fabrics record the focused upward transport of melt through the mush, with the shear stress along the melt-mush interface leading to the alignment of the crystal framework surrounding the melt channel (36, 42, 82).

In summary, melt transport in the mid-ocean ridge crystal mush occurs both by porous and focused flow. Porous flow is an inevitable consequence of crystal mush systems, and, because porous flow is reactive, has major implications for melt evolution. It is supplemented by rapid, channelised flow that results from a combination of replenishment and the concentration of interstitial melts in the mush into melt-rich bodies. These punctuated events are associated with the destabilisation of the crystal mush, may account for the incompatible trace element distributions in MORB, the diversity of its crystal cargo, and vertical fabrics in plutonic rocks.

3.2. Buffering of melt compositions

Fractional crystallisation has long been the paradigm for the differentiation of magmas (87), and this has also been traditionally been invoked to explain the differentiation of MORB (e.g., (88)). However, if melts evolved in a crystal mush rather than a melt-filled magma chamber, fractional crystallisation may be less effective. As outlined in section 3.1, reactions between migrating melts and the cumulus framework may play an important role in the compositional evolution of interstitial melt, and these melts may be remobilised and mixed with replenished melts during melt extraction. The record preserved in oceanic gabbros indicates that these reactions are generally (though not exclusively) between melts that are evolved compared to the melts that formed the framework crystals: much of the associated mineral zonation is normal (34, 54). A second type of reaction that may occur is associated with replenishment: hot, primitive melts are not in equilibrium with lower crustal cumulates, and will induce melting reactions (89-95). Combined, these reactions serve to reduce the compositional variance of the melts in the system; both evolved and primitive melts react with the mush in an attempt to gain equilibrium with it.

In the end member scenario where these two types of reactive process go to completion crystallisation will approach equilibrium crystallisation, forcing all melts onto the 3-phase olivine-plagioclase-clinopyroxene cotectic (assuming that those are the phases in the mush). In this case, melt-mush reaction would buffer all melt compositions, leading to MORB with little major element variability. In nature, full equilibrium is unlikely to be obtained: preserved reaction textures and zoning patterns (e.g., (34, 56, 57, 89)) indicate that reactions do not tend to go to completion.

Furthermore, there is significant small-scale mineralogical and compositional variability in the lower oceanic crust (e.g., (33, 37, 50)). Hence, even if melts achieve local equilibrium with their host, continued migration will lead to disequilibrium once more as they reach the next unit. However, different elements will react at different rates: those for which diffusive exchange is rapid are more likely to attain equilibrium, at least on a local scale, whereas slow diffusing elements require extensive melting and/or dissolution-precipitation reactions and are less likely to attain equilibrium. In this context, it is instructive to look at FeO-MgO relationships: Fe-Mg exchange between olivine and melt is rapid (96), so Fe-Mg is the best candidate for examining a potential role of the crystal mush in buffering melt compositions. That Fe-Mg buffering occurs during melt porous flow in the mush is clear from the mineral compositions of clinopyroxene in oceanic gabbroic rocks. Some of these, especially those occurring as interstitial grains or oikocrysts in primitive troctolitic cumulates, contain high TiO₂ contents, indicating that they crystallised from evolved melts. However, they have high Mg#, and are in Fe-Mg equilibrium with the surrounding Fo-rich olivine (53). Combined, the textures and compositions indicate that evolved, clinopyroxene-saturated melt percolated the troctolite, acquiring a higher Mg# through equilibration of the host olivine (34, 53). Slow diffusing elements, in this case Ti, reflect the high degree of differentiation of the melt, whereas the fast-diffusing Fe-Mg relationships show an apparent primitive origin as a result of diffusive reequilibration.

In figure 3, we plot histograms of the Mg# of the East Pacific Rise and Mid-Atlantic Ridge glass datasets. These were downloaded from the PetDb database (97, 98), and comprise data for 3825 Pacific and 3607 Atlantic glasses. We calculated Mg# assuming $Fe^{3+}/Fe^T=0.12$. The most striking feature is narrow range present in the distributions: the standard deviations are 4.2 mol% for the Atlantic and 6.2% for the Pacific. The small variation in Mg# in samples representing thousands of kilometres of ridge volcanism indicates that there is a magmatic process that modulates the Fe-Mg systematics of melts extracted from the plumbing system. This could be replenishment-mixing: melt-rich reservoirs undergoing a cyclic evolution of replenishment, tapping and fractionation can reproduce the global MORB MgO distribution (67). Alternatively, the narrow distribution may result from the scenario outlined above, where the reaction of both evolved interstitial and primitive replenishing melts with the mush framework provides a buffering capacity. At the least, the observation of Fe-Mg buffering during reactive flow in the lower oceanic crust indicates that this scenario is a viable one.

Another consideration is the role of temperature. The Pacific glass data have a lower mean Mg# (57.7) than their Atlantic counterparts (61.1), and have a non-Gaussian distribution, characterised by a skew towards the low-Mg# end (Fig. 3). The lower mean Pacific Mg# has been interpreted to reflect the temperature of the underlying magma plumbing system, with slow-spreading magma chambers thought to be more thermally insulated and hotter than fast-spreading magma chambers, leading to a lower mean degree of differentiation (99). The low-Mg# tail has been interpreted to mark either the dying stage of replenished-tapped-fractionated magma chambers (67), or the interaction of melts with cool, hydrothermally altered crust at ridge discontinuities such as propagating ridge tips and overlapping spreading centres (100). Crystal mush processes may provide an alternative explanation for this observation: numerical models of the thermochemical evolution of crystal mush show that one of the consequences of melt migration through a mush results in the collection of relatively cool, evolved melts at the top of the section; hence, the mush becomes stratified with respect to temperature and composition (62). These model predictions match remarkably well with the mineral compositional profile of the Pacific lower crust at Hess Deep, which shows an upward differentiation trend, with the uppermost gabbroic rocks representing crystallisation from highly evolved melts (54, 59). Furthermore, seismic data indicate that the crystal mush is most (vertically) extensive at fast-spreading ridges compared to slow-spreading ridges (see section 2); hence, it would be predicted to develop more advanced compositional stratification. The result, then, is that Pacific lavas have, on average, a lower Mg#, and that they extend to lower Mg#, than slower-spreading lavas.

3.3. Cryptic fractionation: the clinopyroxene paradox

It has long been recognised that a large majority of MORB have major element trends indicative of fractionation of clinopyroxene, which is particularly manifest in a decrease in CaO with decreasing MgO (101). However, clinopyroxene phenocrysts are rare, and experimental data indicate that many MORB are not saturated in clinopyroxene at low pressure (102, 103). This issue has been referred to as the pyroxene paradox (69, 104).

Although the pyroxene paradox has been recognised for decades, it has largely remained a qualitative concept. There are very few large MORB suites for which both mineral modes of phenocryst phases, required to quantify the abundance of clinopyroxene, and major element data, to test for clinopyroxene fractionation, are available. To address this, we have collected modal

proportions of phenocrysts from mid-ocean ridge basalts from the Gakkel Ridge (Arctic Ocean). The Gakkel Ridge is the slowest-spreading mid-ocean ridge on Earth, with spreading rates decreasing westwards from 14.6 mm yr⁻¹ to 6.3 mm yr⁻¹ (105). Because the rate of mantle upwelling scales with spreading rate, the magnitude of mantle melting and heat advection to the oceanic crust at ultraslow spreading rates is lowest. As a result, crustal thickness is significantly reduced, whereas lithospheric thickness is increased (106). At Gakkel, lithospheric thickness has been estimated to be as much as 35 km (107). Hence, for the purpose of examining the pyroxene paradox, Gakkel Ridge is a good candidate: with the lithosphere being thick, melt evolution might occur at elevated pressures compared to slow- and fast-spreading ridges, leading to increased stability of clinopyroxene (e.g., (88, 108, 109)). If clinopyroxene is rare even under these conditions, which favour its crystallisation, this would suggest that there is an intrinsic process in the mid-ocean ridge plumbing system which prevents much of the clinopyroxene that has crystallised to be erupted as phenocrysts.

The Gakkel Ridge basalts studied herein were collected during the international Arctic MOR Expedition (AMORE 2001: (110)) and sample ~850 km of the ridge axis. Samples were collected from different tectonomagmatic segments of the ridge to ensure a good representation of Gakkel MORB as a whole (see (110) for details on tectonomagmatic segmentation). To obtain mineral modes, element maps of 95 samples were obtained, which were subsequently transformed into phase maps (see Methods in the Supplementary data for details).

The result of our modal analysis is presented in Supplementary Table S2 and illustrated in figure 4. The average modal proportion of Gakkel basalt phenocrysts is 8.5% plagioclase, 2.1% olivine and 0.1% clinopyroxene (Fig. 4b). Of the 95 samples studied, 94 contain olivine phenocrysts, 62 contain plagioclase, and 13 contain clinopyroxene (Fig. 4a): this amounts to 99%, 65% and 14% of the sample set, respectively. Whereas olivine and most of the plagioclase occur as individual crystals, there are only three samples in which clinopyroxene occurs simply as phenocrysts: in the majority of clinopyroxene-bearing samples, clinopyroxene phenocrysts occur alongside glomerocrysts of intergrown clinopyroxene and plagioclase (Fig. 5). One sample contains clinopyroxene only as plagioclase-clinopyroxene glomerocrysts. A detailed textural study of these glomerocrysts indicates that they represent fragments of crystal mush that was entrained in the basalt prior to eruption (Bennett et al., in prep).

In order to test whether the Gakkel basalts contain a chemical imprint of clinopyroxene fractionation, we have examined their MgO-CaO relationships. For this purpose, we have compiled all Gakkel glass analyses (n=516) from the literature (110-116). In order to relate the compositions of

the literature data to the modal data on our samples, we also present new glass data on a subset (n=34) of our Gakkel samples (Supplementary Table S3; see Supplement for methods). Our new glass data overlap the literature data, indicating that our samples, for which modal data are available, are representative of the broader Gakkel melt compositions.

The MgO-CaO relationships are shown in figure 6. As is typical for MORB (e.g., (117)), the data form a broad array with a positive slope (i.e., decreasing CaO with decreasing MgO), with significant variation at the high CaO end. We superimpose the low-pressure liquid lines of descent of two of the primitive Gakkel glasses, which we modelled using rhyolite MELTS v. 1.2 (32), assuming a pressure of 0.1 kbar and oxygen fugacity of QFM-1. It is immediately clear that the data do not represent a simple cogenetic suite, as those primitive samples with relatively high CaO (>~11.2 wt%, including prominent groups at 11.4 wt%, 11.7 wt% and 12.0 wt%) cannot be produced by crystallisation of the most primitive of the glasses, which are characterised by relatively low CaO (~11 wt%). Hence, there is clear variation in the glass data related to the composition and/or degree of melting of the mantle source. It is beyond the scope of this paper to reconstruct the detailed petrogenetic history of the Gakkel glasses; nonetheless, the liquid lines of descent are informative when it comes to assessing clinopyroxene fractionation, because the olivine and olivine+plagioclase sections of the liquid lines of descent form essentially horizontal arrays. The only way for melts to get decrease in CaO is through clinopyroxene fractionation. At low pressure, this will occur relatively late, as is illustrated in figure 6. With increasing pressure, clinopyroxene will saturate earlier, at higher MgO contents. As such, the low-pressure olivine and olivine+plagioclase parts of the liquid lines of descent form the maximum upper boundary between clinopyroxene-saturated and clinopyroxene-undersaturated melts (e.g., (117)). The observation that nearly all of the glasses fall below this boundary for the high-CaO starting composition, and a large majority do so for the low-CaO starting composition, indicates that, like global MORB (67), most of the Gakkel glasses have a geochemical signature of clinopyroxene crystallisation. Hence, the combined modal and compositional data indicate that the pyroxene paradox applies to the Gakkel Ridge: many of the samples have crystallised clinopyroxene, but only 14% contain clinopyroxene, and clinopyroxene on average only forms 0.1% of the phenocryst mode.

A number of different mechanisms have been proposed to account for the pyroxene paradox. One relates to MORB phase equilibria, which are such that, at increasing pressure, the clinopyroxene stability field increases (88, 108, 109). Hence, MORB may be saturated at the depth of its source magma chamber, but be undersaturated in clinopyroxene upon eruption onto the seafloor (88, 102, 118). This scenario explains why MORB are commonly undersaturated in clinopyroxene; however, it

does not readily explain why clinopyroxene should not occur as phenocrysts. Although some resorption of clinopyroxene phenocrysts could occur during melt transport from the magma reservoir to the seafloor, the rapid transport during dyking events makes it unlikely that nearly all clinopyroxene should be assimilated back into the melt. An alternative, that density separation of clinopyroxene ($\rho \sim 3.25 \text{ gr/cm}^3$) from plagioclase ($\rho \sim 2.65 \text{ gr/cm}^3$) occurs during melt transport, is ruled out by the observation that olivine phenocrysts, which have a similar density than clinopyroxene, are common (Fig. 4). A second explanation for the pyroxene paradox is provided by magma mixing (68). If evolved, clinopyroxene-saturated melts mix with primitive, clinopyroxene-undersaturated melts during replenishment events, the resulting mixture will be clinopyroxene-undersaturated. It will, however, have lower CaO at a given MgO than the olivine-plagioclase control line, because the evolved melt will have crystallised clinopyroxene prior to mixing, lowering its CaO content. A similar scenario could be envisaged during in-situ fractionation (73), where evolved, clinopyroxene-saturated melts are extracted from crystal-rich portions of the magma chamber and are added back to the main melt reservoir.

Crystal mush offers an alternative explanation to these scenarios (53). When primitive MORB is emplaced in the lithosphere (be it the mantle lithosphere at (ultra)slow-spreading ridges or the lower crust at fast-spreading ridges) it will start crystallising. The first increments of crystallisation are olivine, quickly followed by olivine+plagioclase. At the point where plagioclase joins the liquidus, the crystallisation rate increases dramatically (119). As a result, the magma turns into mush as a crystal framework starts forming. At what proportion of crystals a framework starts forming has been the subject of considerable recent interest. This so-called critical crystal volume fraction (Φ_c) is not simply a function of the crystallinity, but also depends on grain shape, degree of particle alignment, surface roughness and melt viscosity (120, 121). Hence, there is no unique value of Φ_c : it differs from one system to the next, and within the system as any of these parameters change (120). Another key aspect is that, even at relatively high melt proportion, crystals may form force chains that can sustain yield strength (120, 122). A consequence of force chains is that the mechanical transition from melt to mush occurs at relatively low crystal proportions (122). At mid-ocean ridges, that fact that crystallisation is dominated by plagioclase, which has a large degree of shape anisotropy, promotes low Φ_c (121) and hence early mush formation: natural and experimental observations suggest that plagioclase-dominated systems may behave mechanically like a mush at relatively low crystal content ($\sim 20\text{-}25\%$; (121, 122)). Such modal proportion is strikingly similar to the fraction of crystals that has formed from mid-ocean ridge basalts at lower crustal pressure by the time it reaches

clinopyroxene saturation (22% in the Indian MORB modelled in section 3.1; see Fig. 13 in (34)). Hence, by the time clinopyroxene crystallises, it does so within an olivine+plagioclase framework. Average MORB possesses a Mg# of ~60 (though slightly higher at slow-spreading compared to fast-spreading ridges (99)), which requires ~40-50% fractionation of a primary melt (Mg#~72). Hence, given that a framework already forms at 20-25% crystallisation, a significant proportion of MORB crystallisation is likely to occur in this framework-dominated mode, rather than in a melt-dominated mode. The implication is that, being an interstitial phase in a crystal framework, clinopyroxene does not crystallise as a 'free' phase within a pure magma, as models based on melt-filled magma chambers would predict. Hence, clinopyroxene does not readily form phenocrysts suspended in a magma-rich reservoir, and is thus unlikely to erupt: it is essentially trapped in the mush. Nonetheless, melts extracted from the mush will show a chemical signature of clinopyroxene crystallisation.

It is difficult to identify parameters that uniquely discriminate between the different explanations for the pyroxene paradox, and in fact the paradox might result from a combination of the different processes discussed above. Nonetheless, three arguments suggest that the mush explanation is a viable one. First, the Gakkel lavas contain few clinopyroxene phenocrysts despite the conditions favouring relatively high-pressure fractionation: hence, there must be something in the magma plumbing system that prevents them from being erupted. Second, ultraslow-spreading ridges are relatively magma poor, and contain no documented melt-rich magma chambers, limiting the opportunity for magma mixing. Instead, slow- and ultraslow-spreading magma plumbing systems are dominated by crystal mush, providing ample opportunity for clinopyroxene to get trapped in a mush. Third, clinopyroxene in oceanic plutonic rocks commonly grows around or in between idiomorphic plagioclase (e.g., (123)). Three examples from the longest recovered section of lower oceanic crust (Hole 735B, Indian Ocean) are shown in figure 7. Although each example has different modal proportions and grain size, they each contain lath-shaped plagioclase that forms a network. Clinopyroxene grows either as minor interstitial phase defining an intergranular texture (Fig. 7a), or fills in a larger proportion of the pore space, growing in between and around plagioclase laths in a subophitic manner (Fig. 7b,c). We take these textures as indications that clinopyroxene crystallised within the framework of previously crystallised olivine+plagioclase. Such textures bear a striking resemblance to the glomerocrysts in the Gakkel basalts, where clinopyroxene also forms within a plagioclase framework (Fig. 5). These samples provide a direct snapshot of the crystal mush, illustrating that the formation of plagioclase frameworks, and subsequent interstitial growth of clinopyroxene is an important step in the evolution of melts emplaced in the lower oceanic crust.

4. Synthesis

In figure 8, we present our observations and interpretations in the form of a schematic cartoon illustrating the processes operating in lower oceanic crustal crystal mush systems. This cartoon is deliberately not placed in the context of a fast-spreading or slow-spreading ridge: we view the processes we describe as generic to any crystal mush, irrespective of context.

We highlight a number of features. The first is the role of replenishment of melts derived from the upper mantle. Replenishment will lead to the formation of melt-rich lenses in the crystal mush (melt lens 1 in figure 8). Along the margins of these lenses two processes will operate: partial melting of the surrounding crystals, and mixing of the replenishing melt with the interstitial melt of the surrounding mush. Both processes lead to homogenisation of the melts ultimately extracted from the crystal mush. The mixing process of interstitial melts into the replenishing melt will achieve a geochemical signature similar to in-situ crystallisation, which has been called upon to explain the incompatible trace element distributions of MORB.

As emplaced melts crystallise, plagioclase forms a crystal framework after only limited amounts of crystallisation (20-25%). As a result, clinopyroxene tends to crystallise within a plagioclase-dominated framework, rather than in a melt-filled reservoir, which is consistent with the textures of oceanic plutonic rocks (figure 7). Clinopyroxene is thus rare as phenocryst in MORB, despite the near-ubiquitous signature of its fractionation in MORB evolution.

Throughout the crystal mush, interstitial melts migrate through porous flow, driven by a combination of buoyancy and compaction (figure 8). That compaction, aided by deformation in places, plays a role is suggested by the microtextures of oceanic plutonic rocks (figure 2). Because equilibrium between migrating melts and surrounding crystals is unlikely to be the norm, porous flow is reactive. This leads to a wealth of reaction textures and compositions in oceanic plutonic rocks, and melt evolution trends that are characterised by strong incompatible trace element enrichment relative to fractional crystallisation models. Interstitial melt may segregate to form a second type of melt lens (labelled 2 in figure 8) and thus self-organise into potentially eruptible bodies. This provides an additional mechanism for interstitial melts to contribute to MORB, in addition to mixing along the margins of melt-rich bodies. In the case of interstitial melts migrating by reactive porous flow, the melts may carry a reactive geochemical signature. This provides an alternative explanation for the incompatible trace element distributions of MORB.

Melt-rich lenses may destabilise, facilitating the rapid, channelised upward transport of melt (melt lens 3 in figure 8). This will enable more mixing and reaction to occur between melts in the channel and interstitial melt of the mush around the channel wall. Furthermore, melts in the channel may pick up a range of crystals and glomerocrysts (figures 4, 5) from the channel walls, accounting for the diverse nature of crystal cargo in MORB. Plagioclase crystals along the channel margin may align, forming foliations and lineations in the surrounding mush.

The integrated end result of these various processes is the extraction of melts that are relatively homogeneous in terms of major elements (particularly of rapidly diffusing elements; e.g., Fe-Mg; figure 3), have a cryptic fractionation signature, and carry clear signature of magma mixing. However, magma mixing is accomplished in a very different way to that classically assumed to occur in melt-rich magma chambers: it occurs between melt-rich bodies and the interstitial melts of the crystal mush as melts are emplaced, segregated, and transported by channelised flow. Ultimately, this leads to trace element distributions that are incompatible with fractional crystallisation: the more incompatible elements are over-enriched.

We conclude that the fact that the mid-ocean ridge plumbing system is dominated by crystal mush has a number of fundamental implications for the behaviour and evolution of the system as a whole. Because all of the underlying processes are governed by physical processes, and by the chemical response of the system to these physical processes, we anticipate that the results described herein are inherent to the evolution of crystal mushes in general, irrespective of geodynamic setting. As such, the mid-ocean ridge system can serve as a useful template for trans-crustal mush columns elsewhere.

Additional Information

Data Accessibility

“The datasets supporting this article have been uploaded as part of the Supplementary Material.”

Authors' Contributions

“CJL conceived of the paper, and drafted the manuscript. CJM contributed to critical discussions. ENB analysed the Gakkel samples. All authors read and approved the manuscript”.

Competing Interests

“The author(s) declare that they have no competing interests”.

Funding Statement

This work was supported by a number of NERC grants (particularly NE/I001670/1 to CJL and NE/C509023/1 to CJM). ENB is supported by NERC grant NE/L002434/1.

Acknowledgments

This work represents views developed by the lead author over the last 15 years, and was inspired by discussions with numerous colleagues, in particular Jean Bédard and Henry Dick. We wish to thank Duncan Muir for assistance with the glass analysis, and two anonymous reviewers for their helpful suggestions. This research used samples and/or data provided by the Ocean Drilling Program (ODP). ODP was sponsored by the U.S. National Science Foundation (NSF) and participating countries under management of Joint Oceanographic Institutions (JOI), Inc. The assistance of the staff at the Kochi IODP core repository is gratefully acknowledged.

References

1. Bachmann O, Bergantz GW. On the origin of crystal-poor rhyolites: extracted from batholithic crystal mushes. *Journal of Petrology*. 2004;45(8):1565-82.
2. Cashman KV, Sparks RSJ, Blundy JD. Vertically extensive and unstable magmatic systems: a unified view of igneous processes. *Science*. 2017;355(6331):eaag3055.
3. Cooper KM. What Does a Magma Reservoir Look Like? The “Crystal's-Eye” View. *Elements*. 2017;13(1):23-8.
4. Cann JR. A model for oceanic crustal structure developed. *Geophys JR astr Soc*. 1974;39:169-87.
5. Cann J. New model for the structure of the ocean crust. *Nature*. 1970;226(5249):928.
6. Sinton JM, Detrick RS. Mid-Ocean Ridge magma chambers. *Journal of Geophysical Research*. 1992;97:197-216.
7. Harding AJ, Orcutt JA, Kappus ME, Vera EE, Mutter JC, Buhl P, et al. Structure of young oceanic crust at 13 degrees N on the East Pacific Rise from expanding spread profiles. *Journal of Geophysical Research, B, Solid Earth and Planets*. 1989;94(9):12,163-12,96.
8. Vera EE, Mutter JC, Buhl P, Orcutt JA, Harding AJ, Kappus ME, et al. The structure of 0 to 0.2 m.y. old oceanic crust at 9°N on the East Pacific Rise from expanded spread profiles. *Journal of Geophysical Research*. 1990;95:15,529-15,56.
9. Detrick RS, Buhl P, Vera E, Mutter J, Orcutt J, Madsen J, et al. Multi-channel seismic imaging of a crustal magma chamber along the East Pacific Rise. 1987;326:35-41.
10. Kent GM, Harding AJ, Orcutt JA. Distribution of magma beneath the East Pacific Rise between the Clipperton Transform and the 9 degrees 17'N Deval from forward modeling of common depth point data. *Journal of Geophysical Research, B, Solid Earth and Planets*. 1993;98(8):13,945-13,69.
11. Carbotte SM, Marjanovic M, Carton H, Mutter JC, Canales JP, Nedimovic MR, et al. Fine-scale segmentation of the crustal magma reservoir beneath the East Pacific Rise. *Nature Geosci*. 2013;6(10):866-70.
12. Singh SC, Kent GM, Collier JS, Harding AJ, Orcutt JA. Melt to mush variations in crustal magma properties along the ridge crest at the Southern East Pacific Rise. *Nature*. 1998;394:874-8.
13. Xu M, Pablo Canales J, Carbotte SM, Carton H, Nedimović MR, Mutter JC. Variations in axial magma lens properties along the East Pacific Rise (9°30'N–10°00'N) from swath 3-D

-
- seismic imaging and 1-D waveform inversion. *Journal of Geophysical Research: Solid Earth*. 2014;119(4):2721-44.
14. Marjanović M, Carton H, Carbotte SM, Nedimović MR, Mutter JC, Canales JP. Distribution of melt along the East Pacific Rise from 9°30' to 10°N from an amplitude variation with angle of incidence (AVA) technique. *Geophysical Journal International*. 2015;203(1):1-21.
 15. Hooft EEE, Detrick RS, Kent GM. Seismic structure and indicators of magma budget along the Southern East Pacific Rise. *Journal of Geophysical Research*. 1997;102(B12):27319-40.
 16. Crawford WC, Webb SC, Hildebrand JA. Constraints on melt in the lower crustal and Moho at the East Pacific Rise, 9 degrees 48'N, using seafloor compliance measurements. *Journal of Geophysical Research, B, Solid Earth and Planets*. 1999;104(2):2923-39.
 17. Crawford WC, Webb SC. Variations in the distribution of magma in the lower crust and at the Moho beneath the East Pacific Rise at 9 degrees -10 degrees N. *Earth and Planetary Science Letters*. 2002;203(1):117-30.
 18. Dunn RA, Toomey DR, Solomon SC. Three-dimensional seismic structure and physical properties of the crust and shallow mantle beneath the East Pacific Rise at 9 degrees 30'N. *Journal of Geophysical Research*. 2000;105(10):23,537-23,55.
 19. Marjanovic M, Carbotte SM, Carton H, Nedimovic MR, Mutter JC, Canales JP. A multi-sill magma plumbing system beneath the axis of the East Pacific Rise. *Nature Geosci*. 2014;7(11):825-9.
 20. Canales JP, Carton H, Carbotte SM, Mutter JC, Nedimovic MR, Xu M, et al. Network of off-axis melt bodies at the East Pacific Rise. *Nature Geosci*. 2012;5(4):279-83.
 21. Garmany J. Accumulations of melt at the base of young oceanic crust. *Nature*. 1989;340(6235):628-32.
 22. Canales JP, Singh SC, Detrick RS, Carbotte SM, Harding A, Kent GM, et al. Seismic evidence for variations in axial magma chamber properties along the southern Juan de Fuca Ridge. *Earth and Planetary Science Letters*. 2006;246(3-4):353.
 23. Van Ark EM, Detrick RS, Canales JP, Carbotte SM, Harding AJ, Kent GM, et al. Seismic structure of the Endeavour Segment, Juan de Fuca Ridge: Correlations with seismicity and hydrothermal activity. *Journal of Geophysical Research: Solid Earth*. 2007;112(B2).
 24. Auzende J-M, Bideau D, Bonatti E, Cannat M, Honnorez J, Lagabrielle Y, et al. Direct observation of a section through slow-spreading oceanic crust. *Nature*. 1989;337:726-9.
 25. Lin J, Purdy GM, Schouten H, Sempere J-C, Zervas C. Evidence from gravity data for focused magmatic accretion along the Mid-Atlantic Ridge. *Nature*. 1990;344:627-32.
 26. Cannat M. How thick is the magmatic crust at slow spreading oceanic ridges. *Journal of Geophysical Research*. 1996;101(B2):2847-57.
 27. Sinha MC, Navin DA, MacGregor LM, Constable S, Peirce C, White A, et al. Evidence for accumulated melt beneath the slow-spreading Mid-Atlantic Ridge. *Philosophical Transactions of the Royal Society of London Series A: Mathematical, Physical and Engineering Sciences*. 1997;355(1723):233.
 28. Singh SC, Crawford WC, Carton H, Seher T, Combier V, Cannat M, et al. Discovery of a magma chamber and faults beneath a Mid-Atlantic Ridge hydrothermal field. *Nature*. 2006;442(7106):1029-32.
 29. Canales JP, Collins JA, Escartin J, Detrick RS. Seismic structure across the rift valley of the Mid-Atlantic Ridge at 23 degrees 20' (MARK area); implications for crustal accretion processes at slow spreading ridges. *Journal of Geophysical Research, B, Solid Earth and Planets*. 2000;105(12):28,411-28,25.
 30. Dunn RA, Lekic V, Detrick RS, Toomey DR. Three-dimensional seismic structure of the Mid-Atlantic Ridge (35°N): Evidence for focused melt supply and lower crustal dike injection. *Journal of Geophysical Research*. 2005;110(B09101):doi:10.1029/2004JB003473.

-
31. McKenzie D. The generation and compaction of partially molten rock. *Journal of Petrology*. 1984;25:713-65.
 32. Gualda GA, Ghiorso MS, Lemons RV, Carley TL. Rhyolite-MELTS: a modified calibration of MELTS optimized for silica-rich, fluid-bearing magmatic systems. *Journal of Petrology*. 2012;53(5):875-90.
 33. Dick HJB, Natland JH, Alt JC, Bach W, Bideau D, Gee JS, et al. A Long In-Situ Section of the Lower Ocean Crust: Results of ODP Leg 176 Drilling at the Southwest Indian Ridge. *Earth and Planetary Science Letters*. 2000;179:31-51.
 34. Lissenberg CJ, MacLeod CJ. A Reactive Porous Flow Control on Mid-ocean Ridge Magmatic Evolution. *Journal of Petrology*. 2016;57(11-12):2195-220.
 35. Holness MB, Vukmanovic Z, Mariani E. Assessing the Role of Compaction in the Formation of Adcumulates: a Microstructural Perspective. *Journal of Petrology*. 2017;58(4):643-73.
 36. MacLeod CJ, Boudier G, Yaouancq G, Richter C. Gabbro fabrics from Site 894, Hess Deep: implications for magma chamber processes at the East Pacific Rise. In: Mevel C, Gillis KM, Allan JF, Meyer PS, editors. *Proceedings of the Ocean Drilling Program*. 147. College Station, TX: Ocean Drilling Program; 1996. p. 317-28.
 37. Gillis KM, Snow JE, Klaus A, Abe N, Adriaio AB, Akizawa N, et al. Primitive layered gabbros from fast-spreading lower oceanic crust. *Nature*. 2014;505(7482):204-7.
 38. Ildefonse B, Sokoutis D, Mancktelow NS. Mechanical interactions between rigid particles in a deforming ductile matrix. Analogue experiments in simple shear flow. *Journal of Structural Geology*. 1992;14(10):1253-66.
 39. Meurer WP, Boudreau AE. Compaction of igneous cumulates; Part II, Compaction and the development of igneous foliations. *Journal of Geology*. 1998;106(3):293-304.
 40. Nicolas A, Ildefonse B. Flow mechanism and viscosity in basaltic magma chambers. *Geophysical Research Letters*. 1996;23(16):2013-6.
 41. Nicolas A, Reuber I, Benn K. A new magma chamber model based on structural studies in the Oman Ophiolite. *Tectonophysics*. 1988;151(1-4):87-105.
 42. VanTongeren JA, Hirth G, Kelemen PB. Constraints on the accretion of the gabbroic lower oceanic crust from plagioclase lattice preferred orientation in the Samail ophiolite. *Earth and Planetary Science Letters*. 2015;427:249-61.
 43. Benn K, Allard B. Preferred mineral orientations related to magmatic flow in ophiolite layered gabbros. *Journal of Petrology*. 1989;30(4):925-46.
 44. Perk N, Coogan L, Karson J, Klein E, Hanna H. Petrology and geochemistry of primitive lower oceanic crust from Pito Deep: implications for the accretion of the lower crust at the Southern East Pacific Rise. *Contributions to Mineralogy and Petrology*. 2007;154(5):575-90.
 45. Paterson SR, Vernon RH, Tobisch OT. A review of criteria for the identification of magmatic and tectonic foliations in granitoids. *Journal of structural geology*. 1989;11(3):349-63.
 46. Nicolas A. Kinematics in magmatic rocks with special reference to gabbros. *Journal of Petrology*. 1992;33(4):891-915.
 47. Stevenson DJ. Spontaneous small-scale melt segregation in partial melts undergoing deformation. *Geophysical Research Letters*. 1989;16(9):1067-70.
 48. Holtzman BK, Groebner NJ, Zimmerman ME, Ginsberg SB, Kohlstedt DL. Stress-driven melt segregation in partially molten rocks. *Geochemistry Geophysics Geosystems*. 2003;4:doi:10.1029/2001GC000258.
 49. Bédard JH. Ophiolitic magma chamber processes, a perspective from the Canadian Appalachians. *Layered Intrusions*: Springer; 2015. p. 693-732.

-
50. Blackman DK, Ildefonse B, John BE, Ohara Y, Miller DJ, Abe N, et al. Drilling constraints on lithospheric accretion and evolution at Atlantis Massif, Mid-Atlantic Ridge 30°N. *Journal of Geophysical Research: Solid Earth*. 2011;116(B7):B07103.
 51. Coogan LA, Saunders AD, Kempton PD, Norry MJ. Evidence from oceanic gabbros for porous melt migration within a crystal mush beneath the Mid-Atlantic Ridge. *Geochemistry, Geophysics, Geosystems*. 2000;1(9):doi:10.1029/2000GC000072.
 52. Gao Y, Hoefs J, Hellebrand E, von der Handt A, Snow J. Trace element zoning in pyroxenes from ODP Hole 735B gabbros: diffusive exchange or synkinematic crystal fractionation? *Contributions to Mineralogy and Petrology*. 2007;153(4):429-42.
 53. Lissenberg CJ, Dick HJB. Melt-rock reaction in the lower oceanic crust and its implications for the genesis of mid-ocean ridge basalt. *Earth and Planetary Science Letters*. 2008;271(1-4):311-25.
 54. Lissenberg CJ, MacLeod CJ, Howard KA, Godard M. Pervasive reactive melt migration through fast-spreading lower oceanic crust (Hess Deep, equatorial Pacific Ocean). *Earth and Planetary Science Letters*. 2013;361(0):436-47.
 55. Sanfilippo A, Tribuzio R, Tiepolo M, Berno D. Reactive flow as dominant evolution process in the lowermost oceanic crust: evidence from olivine of the Pineto ophiolite (Corsica). *Contributions to Mineralogy and Petrology*. 2015;170(4):1-12.
 56. Ridley WI, Perfit MR, Smith MC, Fornari DJ. Magmatic processes in developing oceanic crust revealed in a cumulate xenolith collected at the East Pacific Rise, 9 50°N. *Geochemistry, Geophysics, Geosystems*. 2006;7(12):doi:10.1029/2006GC001316.
 57. Gurenko A, Sobolev A. Crust–primitive magma interaction beneath neovolcanic rift zone of Iceland recorded in gabbro xenoliths from Midfell, SW Iceland. *Contributions to Mineralogy and Petrology*. 2006;151(5):495-520.
 58. Kelemen PB, Koga K, Shimizu N. Geochemistry of gabbro sills in the crust-mantle transition zone of the Oman Ophiolite; implications for the origin of the oceanic lower crust. *Earth and Planetary Science Letters*. 1997;146(3-4):475-88.
 59. Lissenberg CJ, Loocke MP, MacLeod CJ. The Paradox of the Axial Melt Lens: Petrology and Geochemistry of the Upper Plutonics at Hess Deep. AGU Fall Meeting; San Francisco 2014. p. Abstract V31B-4733.
 60. Richter FM, McKenzie D. Dynamical models for melt segregation from a deformable matrix. *The Journal of Geology*. 1984;92(6):729-40.
 61. Jackson M, Cheadle M. A continuum model for the transport of heat, mass and momentum in a deformable, multicomponent mush, undergoing solid-liquid phase change. *International journal of heat and mass transfer*. 1998;41(8-9):1035-48.
 62. Solano JMS, Jackson MD, Sparks RSJ, Blundy J. Evolution of major and trace element composition during melt migration through crystalline mush: Implications for chemical differentiation in the crust. *American Journal of Science*. 2014;314(5):895-939.
 63. Burgisser A, Bergantz GW. A rapid mechanism to remobilize and homogenize highly crystalline magma bodies. *Nature*. 2011;471(7337):212.
 64. Schleicher J, Bergantz G. The mechanics and temporal evolution of an open-system magmatic intrusion into a crystal-rich magma. *Journal of Petrology*. 2017;58(6):1059-72.
 65. Spera FJ, Bohron WA. Rejuvenation of crustal magma mush: A tale of multiply nested processes and timescales. *American Journal of Science*. 2018;318(1):90-140.
 66. Bergantz G, Schleicher J, Burgisser A. Open-system dynamics and mixing in magma mushes. *Nature Geoscience*. 2015;8(10):793.
 67. O'Neill HSC, Jenner FE. The global pattern of trace-element distributions in ocean floor basalts. *Nature*. 2012;491(7426):698-704.

-
68. Rhodes JM, Dungan MA, Blanchard DP, Long PE. Magma mixing at mid-ocean ridges: evidence from basalts drilled near 22°N on the Mid-Atlantic Ridge. *Tectonophysics*. 1979;55:35-61.
 69. Dungan MA, Rhodes JM. Residual glasses and melt inclusions in basalts from DSDP Legs 45 and 46: evidence for magma mixing. *Contributions to Mineralogy and Petrology*. 1978;67:417-31.
 70. Shorttle O. Geochemical variability in MORB controlled by concurrent mixing and crystallisation. *Earth and Planetary Science Letters*. 2015;424:1-14.
 71. Walker D, Shibata T, DeLong SE. Abyssal tholeiites from the Oceanographer Fracture Zone. *Contributions to Mineralogy and Petrology*. 1979;70:111-25.
 72. Goss AR, Perfit MR, Ridley WI, Rubin KH, Kamenov GD, Soule SA, et al. Geochemistry of lavas from the 2005–2006 eruption at the East Pacific Rise, 9°46'N–9°56'N: Implications for ridge crest plumbing and decadal changes in magma chamber compositions. *Geochemistry, Geophysics, Geosystems*. 2010;11(5).
 73. Langmuir CH. Geochemical consequences of *in situ* crystallization. *Nature*. 1989;340:199-205.
 74. Moore A, Coogan L, Costa F, Perfit M. Primitive melt replenishment and crystal-mush disaggregation in the weeks preceding the 2005–2006 eruption 9° 50' N, EPR. *Earth and Planetary Science Letters*. 2014;403:15-26.
 75. Colman A, Sinton JM, Rubin KH. Magmatic Processes at Variable Magma Supply along the Galápagos Spreading Center: Constraints from Single Eruptive Units. *Journal of Petrology*. 2016;57(5):981-1018.
 76. Costa F, Coogan LA, Chakraborty S. The time scales of magma mixing and mingling involving primitive melts and melt–mush interaction at mid-ocean ridges. *Contributions to Mineralogy and Petrology*. 2010;159(3):371-87.
 77. Coogan LA, O'Hara MJ. MORB differentiation: In situ crystallization in replenished-tapped magma chambers. *Geochimica et Cosmochimica Acta*. 2015;158:147-61.
 78. Pan Y, Batiza R. Magmatic processes under mid-ocean ridges: A detailed mineralogic study of lavas from East Pacific Rise 9° 30' N, 10° 30' N, and 11° 20' N. *Geochemistry, Geophysics, Geosystems*. 2003;4(11).
 79. Lange AE, Nielsen RL, Tepley FJ, Kent AJR. Diverse Sr isotope signatures preserved in mid-oceanic-ridge basalt plagioclase. *Geology*. 2013;41(2):279-82.
 80. Passmore E, Maclennan J, Fitton G, Thordarson T. Mush Disaggregation in Basaltic Magma Chambers: Evidence from the ad 1783 Laki Eruption. *Journal of Petrology*. 2012;53(12):2593-623.
 81. Boudier F, Nicolas A, Ildefonse B. Magma chambers in the Oman Ophiolite; fed from the top and the bottom. *Earth and Planetary Science Letters*. 1996;144(1-2):239-50.
 82. MacLeod CJ, Yaouancq G. A fossil melt lens in the Oman Ophiolite; implications for magma chamber processes at fast spreading ridges. *Earth and Planetary Science Letters*. 2000;176(3-4):357-73.
 83. Quick JE, Denlinger RP. Ductile deformation and the origin of layered gabbro in ophiolites. *Journal of Geophysical Research*. 1993;98(B8):14015-29.
 84. Phipps Morgan J, Chen Y. The genesis of ocean crust: magma injection, hydrothermal circulation and crustal flow. *Journal of Geophysical Research*. 1993;98:6283-97.
 85. Henstock TJ, Woods AW, White RS. The accretion of oceanic crust by episodic sill intrusion. *Journal of Geophysical Research, B, Solid Earth and Planets*. 1993;98(3):4143-61.
 86. Nicolas A, Boudier F, France L. Subsidence in magma chamber and the development of magmatic foliation in Oman ophiolite gabbros. *Earth and Planetary Science Letters*. 2009;284(1-2):76-87.

-
87. Bowen N. The evolution of the igneous rocks. Princeton, N.J.: Princeton University Press; 1928.
 88. Grove TL, Kinzler RJ, Bryan WB. Fractionation of mid-ocean ridge basalt (MORB). In: Phipps Morgan J, Blackman DK, Sinton JM, editors. Mantle Flow and Melt Generation at Mid-Ocean Ridges. Geophysical Monograph. 71. Washington, D.C.: American Geophysical Union; 1992. p. 281-310.
 89. Bédard JH, Hebert R. The lower crust of the Bay of Islands ophiolite, Canada: Petrology, mineralogy, and the importance of syntexis in magmatic differentiation in ophiolites and at ocean ridges. *Journal of Geophysical Research*. 1996;101(B11):25,105-25,24.
 90. Bédard J. Parental magmas of the Nain Plutonic Suite anorthosites and mafic cumulates: a trace element modelling approach. *Contributions to Mineralogy and Petrology*. 2001;141(6):747-71.
 91. Leuthold J, Lissenberg CJ, O'Driscoll B, Karakas O, Falloon T, Klimentyeva DN, et al. Partial Melting of Lower Oceanic Crust Gabbro: Constraints From Poikilitic Clinopyroxene Primocrysts. *Frontiers in Earth Science*. 2018;6(15).
 92. Kvassnes A, Grove T. How partial melts of mafic lower crust affect ascending magmas at oceanic ridges. *Contributions to Mineralogy and Petrology*. 2008;156:49-71.
 93. Coumans JP, Stix J, Clague DA, Minarik WG, Layne GD. Melt-rock interaction near the Moho: Evidence from crystal cargo in lavas from near-ridge seamounts. *Geochimica et Cosmochimica Acta*. 2016;191:139-64.
 94. Danyushevsky LV, Perfit MR, Eggins SM, Falloon TJ. Crustal origin for coupled 'ultra-depleted' and 'plagioclase' signatures in MORB olivine-hosted melt inclusions: evidence from the Siqueiros Transform Fault, East Pacific Rise. *Contributions to Mineralogy and Petrology*. 2003;144:619-37.
 95. Eason DE, Sinton JM. Lava shields and fissure eruptions of the Western Volcanic Zone, Iceland: Evidence for magma chambers and crustal interaction. *Journal of Volcanology and Geothermal Research*. 2009;186(3-4):331-48.
 96. Chakraborty S. Rates and mechanisms of Fe-Mg interdiffusion in olivine at 980°-1300°. *Journal of Geophysical Research*. 1997;102(B6):12,317-12,31.
 97. Class C, Lehnert K. PetDB Expert MORB (Mid-Ocean Ridge Basalt) Compilation. EarthChem Library2012.
 98. Lehnert K, Su Y, Langmuir CH, Sarbas B, Nohl U. A global geochemical database structure for rocks. *Geochem Geophys Geosyst*. 2000;1(5):1-14.
 99. Rubin KH, Sinton JM. Inferences on mid-ocean ridge thermal and magmatic structure from MORB compositions. *Earth and Planetary Science Letters*. 2007;260(1-2):257-76.
 100. Wanless VD, Perfit MR, Ridley WI, Klein E. Dacite Petrogenesis on Mid-Ocean Ridges: Evidence for Oceanic Crustal Melting and Assimilation. *Journal of Petrology*. 2010;51(12):2377-410.
 101. Cann JR. Major element variations in ocean floor basalts. *Philosophical Transactions of the Royal Society of London Series A, Mathematical and Physical Sciences*. 1971;268:495-505.
 102. Bender JF, Hodges FN, Bence AE. Petrogenesis of basalts from the Project FAMOUS Area: Experimental study from 0-15 kbars. *Earth and Planetary Science Letters*. 1978;41:277-302.
 103. Bence A, Baylis D, Bender J, Grove T. Controls on the Major and Minor Element Chemistry of Mid-Ocean Ridge Basalts and Glasses. In: Talwani M, Harrison C, Hayes D, editors. Deep drilling results in the Atlantic Ocean: ocean crust1979. p. 331-41.
 104. Francis D. The pyroxene paradox in MORB glasses—a signature of picritic parental magmas? *Nature*. 1986;319:586.

-
105. DeMets C, Gordon RG, Argus DF, Stein S. Effect of recent revisions to the geomagnetic reversal time scale on estimates of current plate motions. *Geophysical Research Letters*. 1994;21:2191-4.
 106. Dick HJB, Lin J, Schouten H. An ultraslow-spreading class of ocean ridge. *Nature*. 2003;426:405-12.
 107. Schlindwein V, Schmid F. Mid-ocean-ridge seismicity reveals extreme types of ocean lithosphere. *Nature*. 2016;535(7611):276.
 108. O'Hara MJ. The bearing of phase equilibria studies in synthetic and natural systems on the origin and evolution of basic and ultrabasic rocks. *Earth-Sci Rev*. 1968;4:69-133.
 109. Presnall DC, Dixon SA, Dixon JR, O'Donnell TH, Brenner NL, Schrock RL, et al. Liquidus phase relations on the join diopside-forsterite-anorthite from 1 atm to 20 kbar: Their bearing on the generation and crystallization of basaltic magma. *Contributions to Mineralogy and Petrology*. 1978;66:203-20.
 110. Michael PJ, Langmuir CH, Dick HJB, Snow JE, Goldstein SL, Graham DW, et al. Magmatic and amagmatic seafloor spreading at the slowest mid-ocean ridge: Gakkel Ridge, Arctic Ocean. *Nature*. 2003;423:956-61.
 111. Goldstein SL, Soffer G, Langmuir CH, Lehnert KA, Graham DW, Michael PJ. Origin of a 'Southern Hemisphere' geochemical signature in the Arctic upper mantle. *Nature*. 2008;453(7191):89.
 112. Nauret F, Snow JE, Hellebrand E, Weis D. Geochemical Composition of K-rich Lavas from the Lena Trough (Arctic Ocean). *Journal of Petrology*. 2011;52(6):1185-206.
 113. Nielsen SG, Shimizu N, Lee CTA, Behn MD. Chalcophile behavior of thallium during MORB melting and implications for the sulfur content of the mantle. *Geochemistry, Geophysics, Geosystems*. 2014;15(12):4905-19.
 114. Wanless VD, Behn MD, Shaw AM, Plank T. Variations in melting dynamics and mantle compositions along the Eastern Volcanic Zone of the Gakkel Ridge: insights from olivine-hosted melt inclusions. *Contributions to Mineralogy and Petrology*. 2014;167(5):1-22.
 115. Graham DW, Michael PJ, Shea T. Extreme incompatibility of helium during mantle melting: Evidence from undegassed mid-ocean ridge basalts. *Earth and Planetary Science Letters*. 2016;454:192-202.
 116. Michael PJ, Graham DW. The behavior and concentration of CO₂ in the suboceanic mantle: inferences from undegassed ocean ridge and ocean island basalts. *Lithos*. 2015;236:338-51.
 117. Herzberg C. Partial crystallization of mid-ocean ridge basalts in the crust and mantle. *Journal of Petrology*. 2004;45(12):2389-405.
 118. Elthon D, Kent RD, Meen JK. Compositional variations of basaltic glasses from the Mid-Cayman Rise spreading center. *Journal of Geophysical Research*. 1995;100(7):12497-512.
 119. Kelemen PB, Aharonov E. Periodic formation of magma fractures and generation of layered gabbros in the lower crust beneath oceanic spreading ridges. In: Buck W, Delaney PT, Karson JA, Lagabriele Y, editors. *Faulting and Magmatism at Mid-Ocean Ridges*. *Geophysical Monograph*. 106. Washington, DC: American Geophysical Union; 1998. p. 267-90.
 120. Bergantz GW, Schleicher JM, Burgisser A. On the kinematics and dynamics of crystal-rich systems. *Journal of Geophysical Research: Solid Earth*. 2017;122(8):6131-59.
 121. Saar MO, Manga M, Cashman KV, Fremouw S. Numerical models of the onset of yield strength in crystal-melt suspensions. *Earth and Planetary Science Letters*. 2001;187(3-4):367-79.
 122. Philpotts AR, Shi J, Brustman C. Role of plagioclase crystal chains in the differentiation of partly crystallized basaltic magma. *Nature*. 1998;395:343.

-
123. Dick HJB, Ozawa K, Meyer PS, Niu Y, Robinson PT, Constantin M, et al. Primary silicate mineral chemistry of a 1.5-km section of very slow spreading lower ocean crust: ODP Hole 735B, Southwest Indian Ridge. In: Natland JH, Dick HJB, Miler DJ, Von Herzen R, editors. Proceedings of the Ocean Drilling Program, Scientific Results. 176. College Station, TX: Ocean Drilling Program; 2002. p. 1-60 [CD-ROM].

Figure captions

Figure 1: Density evolution of a primary MORB, and the cumulates crystallised from it, during progressive fractional crystallisation. Model curves were calculated using MELTS (32), and the primary MORB composition is that of (33) (see Table S1), assuming 0.15% H₂O. The density of the cumulate plotted is the modal proportion multiplied by the density of the phases at each increment of crystallisation: it thus represents the bulk density of the cumulate produced at each step.

Figure 2: Photomicrographs illustrating microtextural evidence for compaction in oceanic cumulates. A. Full thin section scan of troctolite from IODP Hole U1309D at Atlantis Massif (30°N, Mid-Atlantic Ridge). A magmatic foliation, outlined by orange dashed lines, is defined by subparallel plagioclase laths. Plagioclase laths are characterised by tapered deformation twins, with some prominent examples outlined by the white circles. The areas shown in B. and C. are shown by the red boxes. B. and C. Closeups of A., showing a series of kink bands in olivine (outlined by the red arrows) and deformation twins in plagioclase. Ol=olivine; Plag=plagioclase; S1=foliation.

Figure 3: Histograms of Mg#, calculated using $Fe^{3+}/Fe^T=0.12$, for Atlantic (A) and Pacific (B) glass data from the PetDB database (97, 98).

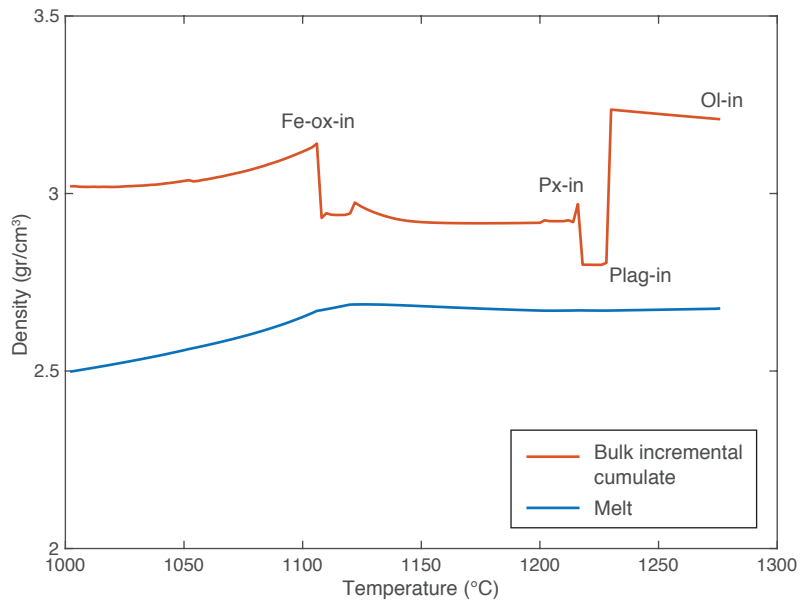
Figure 4: Modal analysis of 95 basalts from the Gakkel Ridge (Arctic Ocean). A. Olivine and plagioclase are present as phenocrysts, but clinopyroxene is not. Within individual samples, clinopyroxene may occur as phenocrysts, glomerocrysts or both. B. Mean modal proportions of phenocrysts in the Gakkel basalts.

Figure 5: Line drawing of glomerocryst in a Gakkel basalt. The glomerocrysts is composed of a network of lath-shaped plagioclase, with granular to interstitial olivine. Clinopyroxene forms anhedral crystals within the plagioclase framework. Scale bar is 1 mm.

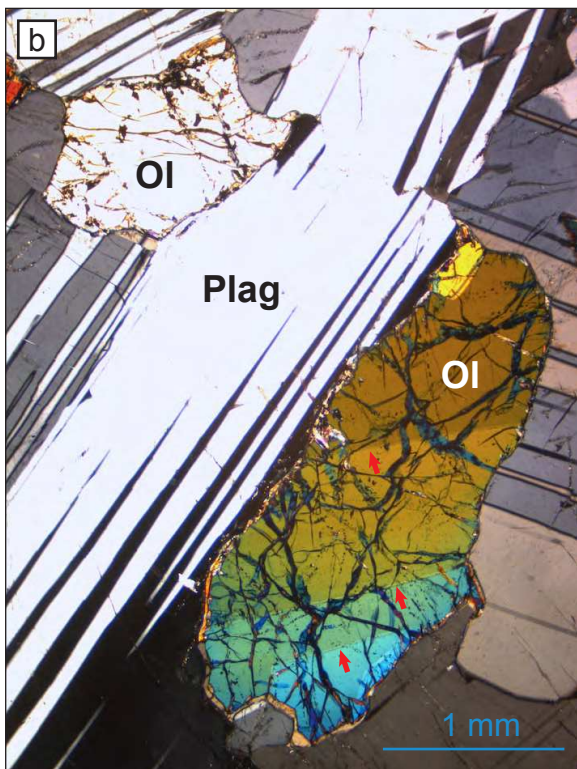
Figure 6: MgO-CaO relationships of glasses from the Gakkel ridge. Literature data (black circles; n=516) are supplemented by 34 new analyses presented herein (green circles; data in Supplementary Table 3). The liquid lines of descent of two primitive glasses, outlined by the blue and red circles, are shown by the solid lines. Water contents were set at 0.25 wt% and 0.4 wt% for the high-CaO and low-CaO primitive melts, respectively. These were chosen on the basis of their location along the Gakkel ridge axis, along with the known along-axis gradient in Gakkel glass water content (114).

Figure 7: Core photographs of gabbroic rocks from OPD Hole 735B (Atlantis Bank, Indian Ocean). A. Fine-grained leucogabbro characterised by interstitial clinopyroxene in a plagioclase network. B. Medium-grained gabbro with higher proportions of clinopyroxene, which grew subophitically to interstitial to a plagioclase network. C. Medium-grained, subophitic gabbro. Despite the higher proportion of clinopyroxene, clinopyroxene still predominantly crystallised within an interconnected framework of plagioclase. Scale bar is 5 cm in each case.

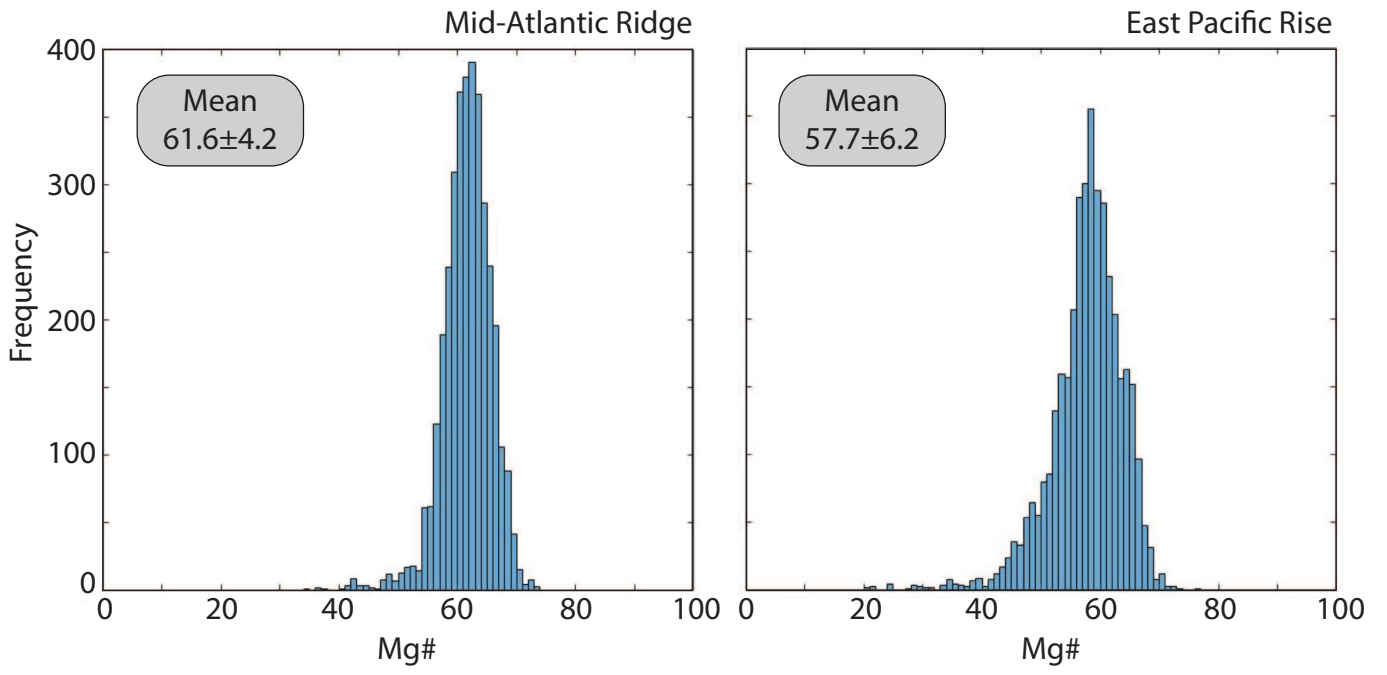
Figure 8: Schematic representation of a lower oceanic crustal crystal mush. Melt lens 1 is formed by replenishment of the crystal mush by primary melt, leading to reaction with the surrounding mush and mixing of interstitial melts into the melt lens. Melt lens 2 forms by the segregation of interstitial melts in the mush. Melt transport occurs both by reactive porous flow, aided by compaction, and by channelised focused flow. The latter, which drains melt lens 3, feeds eruptions of MORB, picking up crystal cargo and producing fabrics in the mush en route.



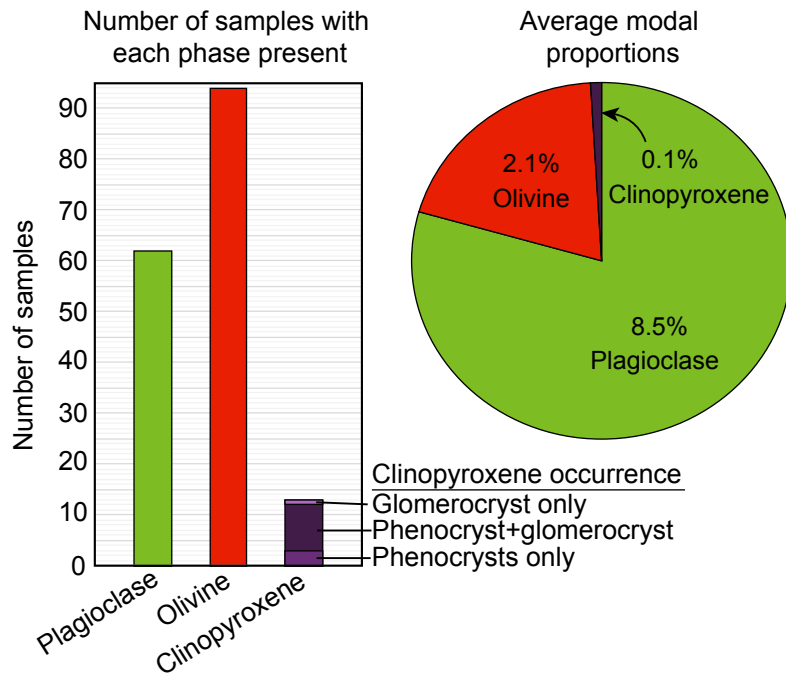
Lissenberg et al., Fig. 1



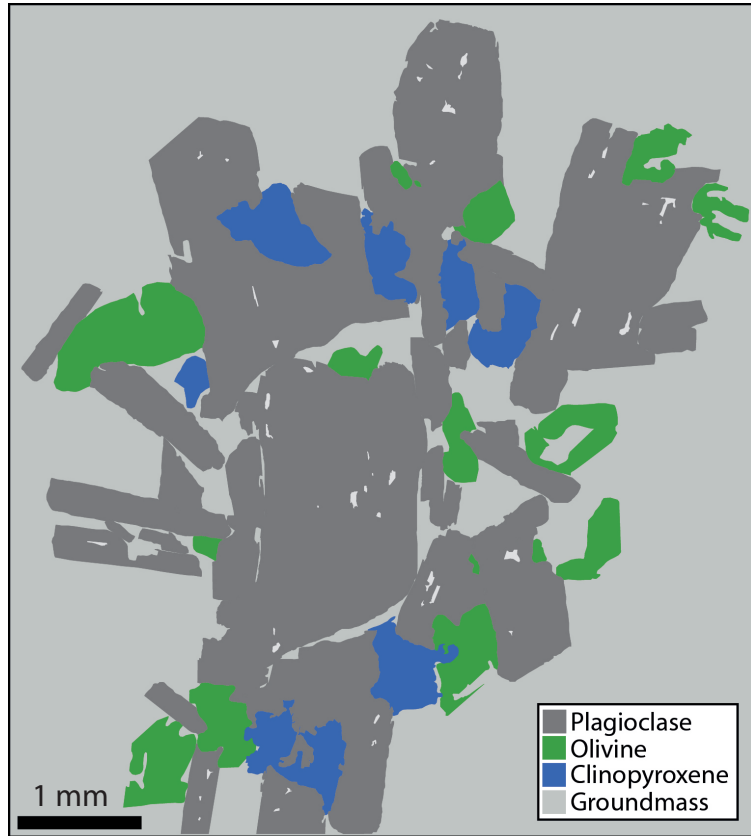
Lissenberg et al., Fig. 2



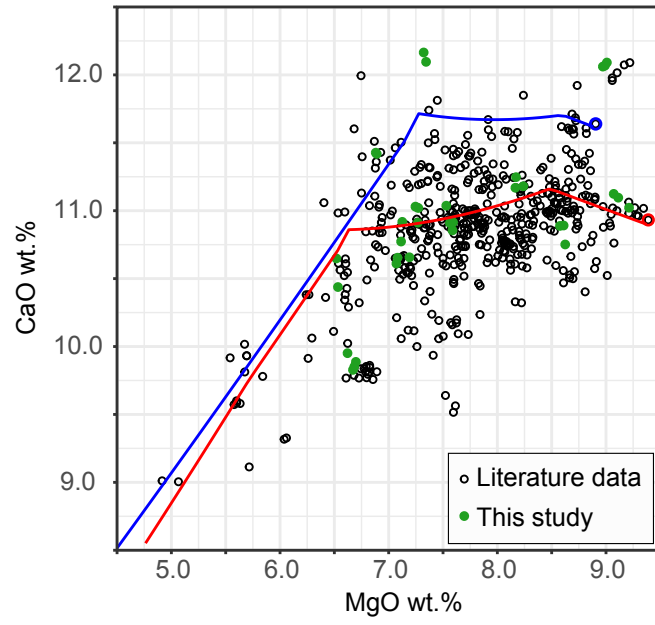
Lissenberg et al., Fig. 3



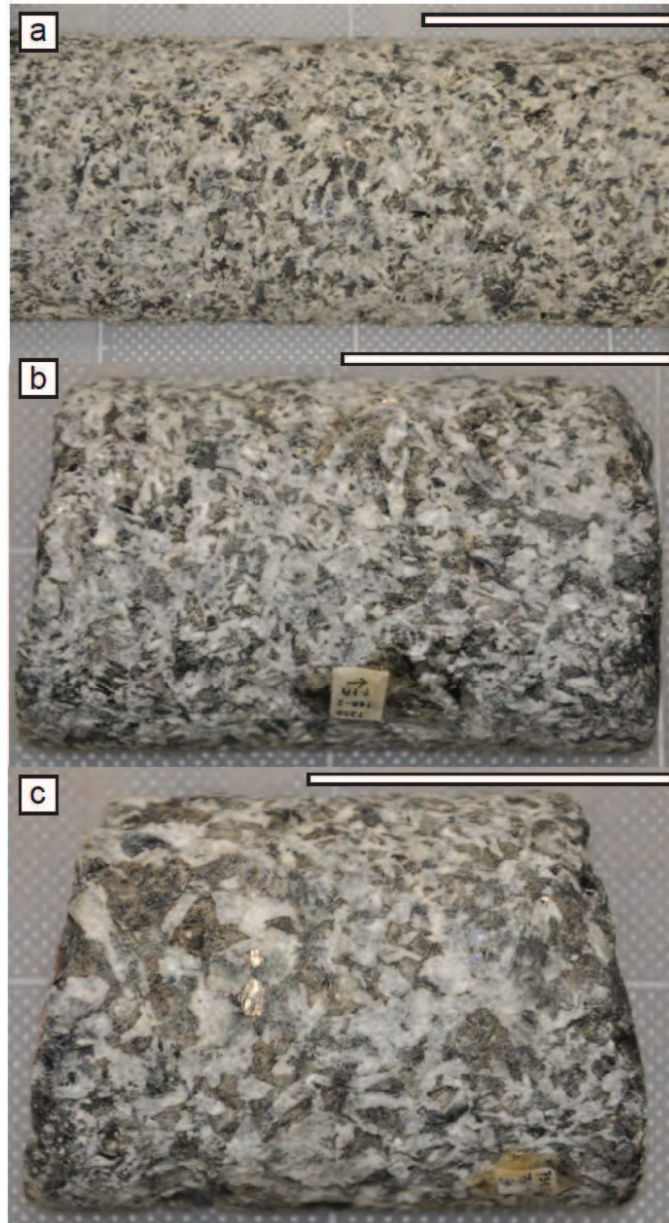
Lissenberg et al., Fig. 4



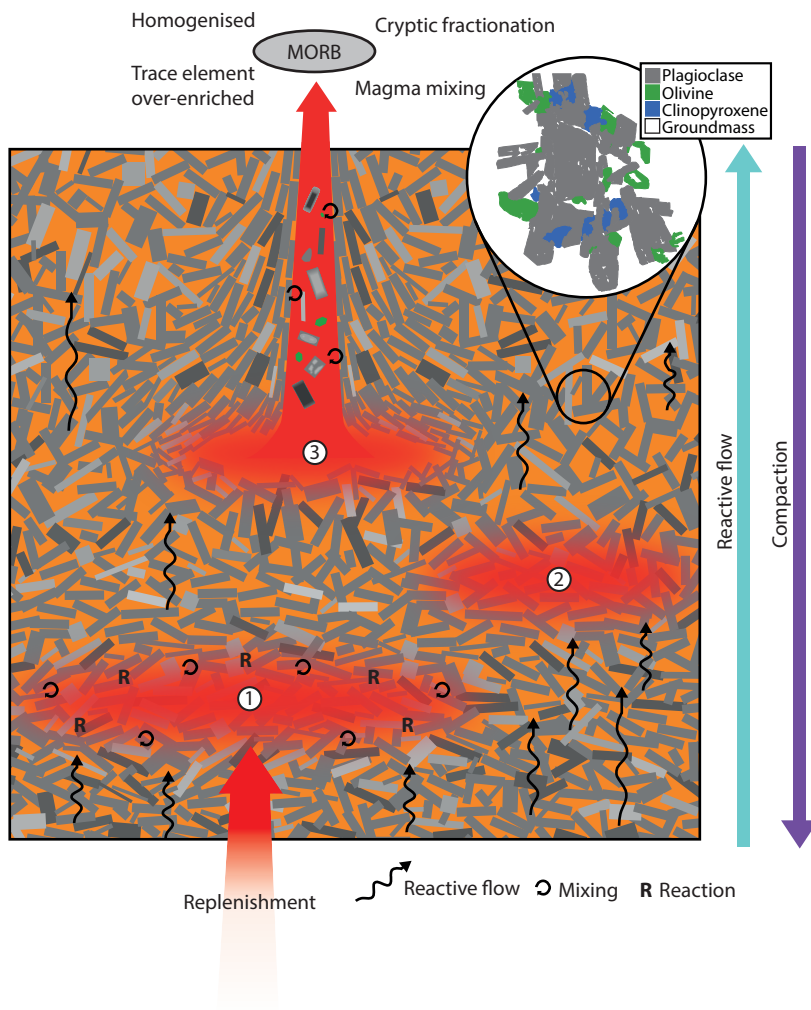
Lissenberg et al., Fig. 5



Lissenberg et al., Fig. 6



Lissenberg et al. figure 7



Lissenberg et al., Fig. 8